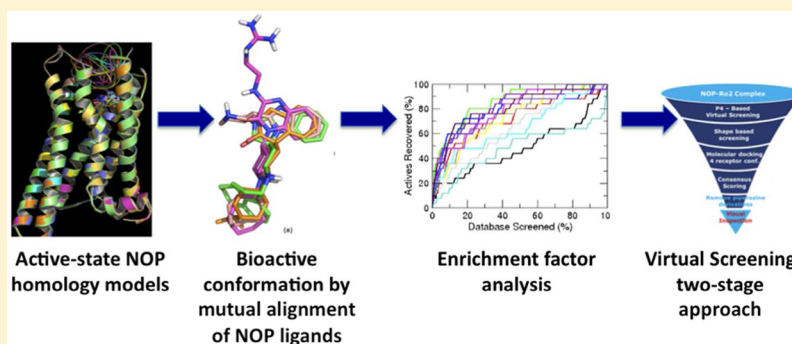


# Structure-Based Virtual Screening of the Nociceptin Receptor: Hybrid Docking and Shape-Based Approaches for Improved Hit Identification

Pankaj R. Daga,<sup>†</sup> Willma E. Polgar,<sup>‡</sup> and Nurulain T. Zaveri<sup>\*,†</sup>

<sup>†</sup>Astraea Therapeutics, LLC., 320 Logue Avenue, Mountain View, California 94043, United States

<sup>‡</sup>SRI International, 333 Ravenswood Avenue, Menlo Park, California 94025, United States



**ABSTRACT:** The antagonist-bound crystal structure of the nociceptin receptor (NOP), from the opioid receptor family, was recently reported along with those of the other opioid receptors bound to opioid antagonists. We recently reported the first homology model of the ‘active-state’ of the NOP receptor, which when docked with ‘agonist’ ligands showed differences in the TM helices and residues, consistent with GPCR activation after agonist binding. In this study, we explored the use of the active-state NOP homology model for structure-based virtual screening to discover NOP ligands containing new chemical scaffolds. Several NOP agonist and antagonist ligands previously reported are based on a common piperidine scaffold. Given the structure–activity relationships for known NOP ligands, we developed a hybrid method that combines a structure-based and ligand-based approach, utilizing the active-state NOP receptor as well as the pharmacophoric features of known NOP ligands, to identify novel NOP binding scaffolds by virtual screening. Multiple conformations of the NOP active site including the flexible second extracellular loop (EL2) loop were generated by simulated annealing and ranked using enrichment factor (EF) analysis and a ligand–decoy dataset containing known NOP agonist ligands. The enrichment factors were further improved by combining shape-based screening of this ligand–decoy dataset and calculation of consensus scores. This combined structure-based and ligand-based EF analysis yielded higher enrichment factors than the individual methods, suggesting the effectiveness of the hybrid approach. Virtual screening of the CNS Permeable subset of the ZINC database was carried out using the above-mentioned hybrid approach in a tiered fashion utilizing a ligand pharmacophore-based filtering step, followed by structure-based virtual screening using the refined NOP active-state models from the enrichment analysis. Determination of the NOP receptor binding affinity of a selected set of top-scoring hits resulted in identification of several compounds with measurable binding affinity at the NOP receptor, one of which had a new chemotype for NOP receptor binding. The hybrid ligand-based and structure-based methodology demonstrates an effective approach for virtual screening that leverages existing SAR and receptor structure information for identifying novel hits for NOP receptor binding. The refined active-state NOP homology models obtained from the enrichment studies can be further used for structure-based optimization of these new chemotypes to obtain potent and selective NOP receptor ligands for therapeutic development.

## INTRODUCTION

The recent availability of high-resolution crystal structures of the four opioid G-protein coupled receptors, viz. the mu, delta, kappa and nociceptin opioid receptors bound to their respective antagonist ligands, provides new opportunities to discover novel opioid receptor binding scaffolds from virtual screening campaigns. From a therapeutic perspective, it is mostly opioid ‘agonists’ that have been most useful for decades as antinociceptive therapies of choice, particularly mu opioid

agonists such as morphine, hydromorphone, oxycodone, and fentanyl. These agonists were discovered through traditional approaches, such as natural product isolation (e.g., morphine), semi-synthetic natural product derivatives (e.g., oxycodone, hydromorphone), and synthetic manipulation of natural product scaffolds (e.g., fentanyl). Even kappa and delta opioid

Received: May 14, 2014

Published: August 22, 2014

receptor agonists are still mostly based on the core natural morphine-like scaffold. On the other hand, ligands for the fourth opioid receptor, the nociceptin receptor (NOP, opioid receptor-like receptor ORL-1), have been discovered by high-throughput screening and other medicinal chemistry approaches because although the NOP receptor belongs to the opioid receptor family, it does not bind most known opioid ligands with appreciable affinity. Therefore, after its discovery in 1994,<sup>1–3</sup> the discovery of small-molecule NOP receptor ligands could not really benefit from the vast chemical library of known opioid ligands already available. Although there have been large number of NOP agonists and antagonists reported in the literature, most NOP receptor ligands, both agonists and antagonists, are based on a common core scaffold, viz. the piperidine ring, whose protonated basic nitrogen has been shown to interact with the highly conserved Asp130 in the TM binding pocket of the NOP receptor GPCR (for reviews on NOP ligands of different chemical classes, see refs 4–7). Most NOP ligand hit-to-lead campaigns have originated from hits discovered via high-throughput screening. There have been no reports of using virtual screening campaigns, either pharmacophore-based or structure-based, in the discovery of NOP ligands. With the recent availability of the crystal structure of the antagonist-bound NOP receptor,<sup>8</sup> it should be possible to expand the chemical universe of NOP receptor ligands into novel chemical entities, perhaps distinct from the common piperidine-based scaffolds. Such endeavors with the other opioid receptors are already being explored through virtual screening (VS) campaigns using the opioid receptor crystal structures.<sup>9</sup>

Studies with receptor chimera and site-directed mutagenesis have shown that in the NOP receptor the second extracellular loop (EL2) loop plays an important role in binding selectivity and activation upon ligand binding, unlike the other three classic opioid receptors.<sup>10,11</sup> While the crystal structure of the activated NOP receptor awaits determination, we recently reported the first homology model of the active-state NOP receptor<sup>12</sup> and showed that EL2 loop residues may interact with bound ligands and undergo activation-associated conformational movements. As part of our ongoing effort to discover NOP receptor ligands containing new chemical scaffolds, the studies described here were focused on utilizing our active-state NOP homology models for structure-based discovery of novel NOP ligands using virtual screening. Given that there are several NOP ligands described in the literature,<sup>4,6,7,13,14</sup> including our own series of NOP ligands,<sup>15,16</sup> we developed a “hybrid” approach in which NOP agonist ligands were used to optimize binding pocket conformations of the active-state NOP receptor. A series of NOP active-state models were then ranked using enrichment factor analysis. The top-ranking models from a combination of these approaches were used in a two-stage virtual screening campaign to discover novel NOP ligand scaffolds.

Structure-based drug design, now an indispensable component of drug discovery, principally employs methods of receptor-based virtual screening and molecular docking for hit identification and lead optimization.<sup>17</sup> Current docking algorithms can successfully handle ligand flexibility in an indisputable manner. However, protein flexibility remains a major challenge during molecular docking-based virtual screening approaches. Current thinking on ligand recognition paradigms has now evolved from Koshland’s classic “induced-fit” mechanism, which assumes that ligand binding induces few

conformational changes in the receptor,<sup>18</sup> to a conformational selection theory, which posits that the ligand binds to a pre-existing receptor conformation from an equilibrated ensemble,<sup>19</sup> after which the ensemble undergoes a population shift. In both scenarios, structural fluctuations of the receptor occur after ligand binding and need to be taken into account during docking studies. Recent developments in high speed processors and newer algorithms have enabled the simultaneous use of molecular docking and protein modeling (especially optimization of side-chains and loops) approaches to address protein flexibility during molecular docking.<sup>20</sup> Another implementation is docking ligands to multiple receptor conformations obtained experimentally by X-ray crystallography or NMR spectroscopy<sup>21</sup> or computationally by molecular dynamics,<sup>22</sup> normal-mode analysis, or other techniques.<sup>23–25</sup> Indeed, an improvement in virtual screening predictive power was recently demonstrated using molecular dynamics snapshots of receptor conformations rather than known crystal structures.<sup>26</sup>

Here, we describe a fast and general *in silico* method for representing the equilibrium dynamics of the receptor binding site, where a small number of conformations of the binding site were generated using simulated annealing, and a few selected conformations (along with the entire receptor) were used in molecular docking studies to locate the best possible receptor conformation for virtual screening. We further illustrate a procedure for refinement of the NOP active-state structure using a shape-based similarity approach in conjunction with molecular docking of several known NOP agonists to arrive at several refined NOP models that provided better enrichment of known actives from a library of decoys than a molecular docking approach alone. A virtual screening campaign using these refined NOP receptor models resulted in identification of several hits containing new chemical scaffolds with reasonable affinity for the NOP receptor. To our knowledge, our efforts represent the first study to find novel hits for the nociceptin opioid receptor using structure-based virtual screening.

## METHODS

**Homology Model of the NOP Receptor.** At the time the homology modeling studies were initiated, Opsin was the only active-state structure available for the GPCR superfamily. Hence, the opsin structure (PDB code: 3CAP) was used as the template for the homology model of the active-state NOP receptor. The model of the inactive-state NOP receptor was constructed by a multiple template approach using the crystal structures of the antagonist-bound inactive  $\beta 2$  adrenergic receptor (AR) (PDB code: 2RH1) and rhodopsin structure (PDB code: 1F88) as templates. Sequence alignment was carried out using ClustalW. The structure alignment was manually adjusted to remove gaps in the helices. The homology models were built using the “Advance Protein Modeling” module in SybylX 1.2. Because the EL2 loop is an integral part of the binding site, extra care was taken to build the EL2 loop. The disulfide bridge between TM3 and EL2 was the second extracellular loop was included in the homology model. After the crude model was constructed, it was subjected to stepwise minimization to remove steric clashes. The sequence of minimization included hydrogen minimization followed by side-chain, backbone, and finally entire receptor minimization. The details of the model building, loop building, and refinement can be found in our previously published report on homology modeling and molecular dynamics simulation of the NOP receptor.<sup>12</sup> The model, validated using PROCHECK

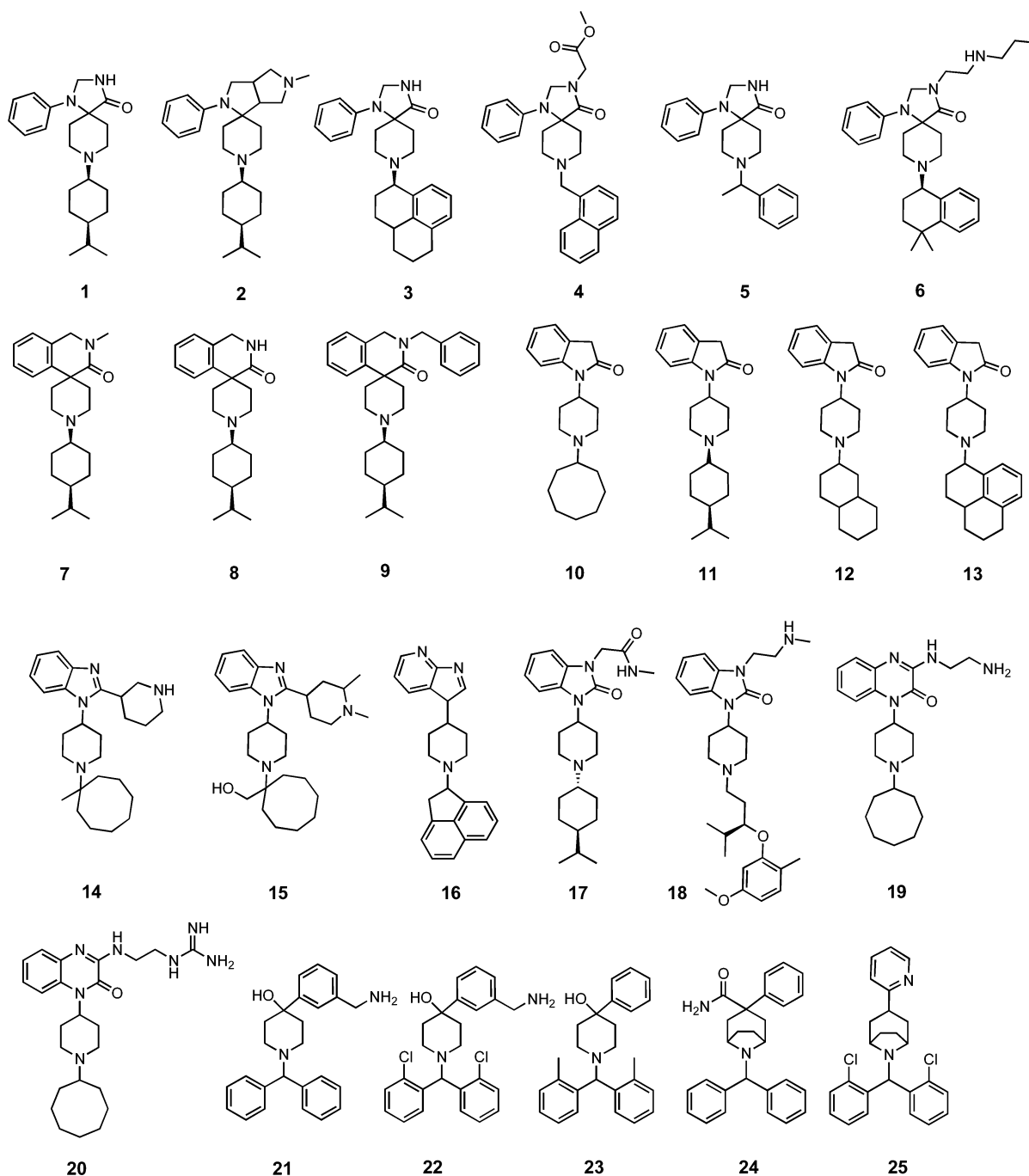


**Figure 1.** NOP receptor agonist ligands used in enrichment studies. Compound numbers and names of the ligands are explained in the text.

and the ProSA Web server, was utilized in this study for the agonist-assisted refinement and selection of receptor conformations for virtual screening and hit identification of new NOP ligands.

**Construction of a Compound Library of NOP Agonists and Drug-like decoys.** A library of 25 NOP receptor agonists (shown in Figure 1) was built. The agonist structures were selected from the literature, reported in various patents and research publications. The selected agonists contained different chemical scaffolds found in known NOP agonist ligands, such as triazaspirodecanone (1–6),<sup>27–30</sup> spiro-isoquinolinones (7–9)<sup>31</sup> oxindoles, (10–13),<sup>15</sup> benzimidazoles (14–18),<sup>32,33</sup> quinazolines (19–20),<sup>34</sup> and phenyl-piperidines (20–25)<sup>35–37</sup> (Figure 1).

Physicochemical properties of the selected agonists were calculated using SybylX 1.2. These properties included molecular weight (MW), number of rotatable bonds (RBs), number of hydrogen bond acceptors (HBAs) and donors (HBDs), and octanol–water partition coefficient (log P). The ranges of these physicochemical properties were used as guidelines for selecting decoys from the ZINC database.

A subset of decoy molecules from ZINC (CNS Permeable subset)<sup>38</sup> was created containing compounds satisfying the following criteria: (i) molecular weight 300–550; (ii) number of rotatable bonds, 2–5; hydrogen bond donors, 1–4, and acceptors, 1–4; (iii) clogP, 2.5–6.5; and (iv) number of rings, 4–6. The filtering, carried out using the “Selector” module in

SybylX 1.2, resulted in a subset of more than 20,000 compounds.

In order to ensure structural diversity among the known NOP ligand set (above) and decoy subset, all decoy candidate compounds with a Tanimoto coefficient ( $T_c$ )  $\geq 0.5$  with respect to any ligand or within the decoy set were removed. The remaining compounds were subjected to clustering on the basis of dissimilarity. A total of 975 compounds were finally selected as decoys.

**Structure-Based Approach. Molecular Docking of NOP Agonist Ro-2 in the Active-State NOP Receptor Model.** Ro-2, a high affinity selective NOP receptor agonist,<sup>39</sup> was docked into the orthosteric site of NOP using Surflex-Dock. Surflex-Dock is based on the Hammerhead fragmentation/reconstruction algorithm to dock compounds into a defined site. The Surflex-Dock protocol is a precomputed molecular representation of an idealized ligand and represents a negative image of the binding site to which putative ligands are aligned.<sup>40</sup> The structure template used for building the active-state NOP homology model did not contain a ligand. Usually, in such a case, it becomes necessary to use available algorithms for finding putative binding pockets. Instead of using such standard site-finding algorithms, we preferred to use the existing knowledge of the NOP binding site from literature mutagenesis studies<sup>41,42</sup> to locate the orthosteric binding site. Since its discovery, a number of mutagenesis studies on the NOP receptor have identified cognate differences between NOP and the other opioid receptors, as well as residues important for binding the endogenous ligand nociceptin. These studies over the years have identified amino acids such as Asp130,<sup>43</sup> Thr305,<sup>41</sup> and Val279<sup>42</sup> to be important for binding of nociceptin. Hence, for this study, the protocol was constructed using a set of active site residues consisting of Tyr58, Asp130, Met134, Val279, Thr305, and Tyr309. Twenty binding poses of Ro-2 were generated and evaluated for possible interactions with binding site.

**Simulated Annealing of the Active Site and EL2 Loop To Generate Receptor Conformations.** In several GPCRs, the second extracellular loop (EL2) is known to function as a lid on top of the receptor binding cavity.<sup>44,45</sup> Similarly, the NOP receptor ligand binding cavity is also capped by EL2 loop residues. The orthosteric binding site is lined by the residues in the EL2 loop situated directly above the binding site. However, this loop is conformationally flexible and mobile during receptor dynamics. Therefore, a significant effort was made here to generate different conformations of the EL2 loop and the orthosteric binding site. The active site was defined as amino acid residues within 7 Å of the docked ligand (Ro-2 in this case) and the entire EL2 loop. Simulated annealing was carried out for the defined active site to generate different conformations. A total of 50 active-site conformations were generated, and each conformation was assessed individually. Each receptor structure was then used for docking studies of the NOP agonist Ro-2 using Surflex-dock. Receptor conformations with the top 12 docking scores and predicted binding poses of Ro-2 were selected for further analysis. The selected 12 receptor models were then used to perform the enrichment studies described below.

**Ligand-Based Approach. Mutual Alignment of NOP Receptor Agonists Using Surflex-Sim.** Surflex-Sim rapidly optimizes the pose of a molecule to maximize 3D similarity to a target molecule. Mutual alignment of multiple molecules generated is referred to as the "hypothesis". The "Hypothesis"

generation tries to find the superposition of all input ligands that maximizes similarity and minimizes the overall volume of the superposition. The mutually aligned conformation of each ligand represents the possible bioactive conformation of that ligand. This process is slow, and the alignment time increases exponentially with the number of ligands in the set. This approach is usually employed in cases where the protein active-site is unavailable. However, because we had already obtained the bioactive conformation of NOP agonists from molecular docking into the NOP active-site (see above), we used this information to generate a manual pharmacophore using four NOP agonists of distinct structural scaffolds from our NOP ligand set (Figure 1). NOP ligands selected for the mutual alignment included triazaspirodecanone Ro-64-6198 (3), spiroisoquinolinone (7), benzimidazole (14), and quinazoline (20).

**Manual Pharmacophore Using Bioactive Conformation of Ro-2.** The bioactive conformation of the Ro-2 was used to define a manual structure-based pharmacophore using Unity in SybylX 1.2. A structure-based pharmacophore possesses an advantage over a ligand-based pharmacophore because one does not need to assume the bioactive conformation; instead, the binding conformation of the ligand is directly used to define the pharmacophoric features. Pharmacophore features were defined using the structure–activity knowledge of the triazaspirodecanone series of NOP ligands. For simplicity, most NOP ligands have molecular characteristics that can be assigned into three main pharmacophoric features: (1) heterocyclic/aromatic "A moiety", (2) basic nitrogen-containing "B moiety", and (3) the lipophilic substitution "C moiety" on the basic nitrogen.<sup>16</sup> The 3D pharmacophore query generated in Unity from Ro-2 contained four features: an aromatic ring, a positive ionizable group at piperidine ring N, and two hydrophobic groups representing the isopropyl–cyclohexyl group. This pharmacophore was used for screening of the CNS Permeable subset (409,874 compounds) of the ZINC database.

**Enrichment Factor Analysis Using the Hybrid Structure-Based and Ligand Shape-Based Approach. Molecular Docking of Agonist-Decoy Library into Various NOP Receptor Active-state Conformations.** The above-mentioned in-house database of 25 NOP receptor agonists and 975 decoys was subjected to molecular docking using the Surflex-Dock module interfaced with SybylX 1.2. Thirteen active-state and one inactive-state NOP receptor conformations were used for the docking analysis. The protocol was defined using the existing ligand (Ro-2) inside the receptor binding site. Docking was performed using the Geom protocol in Surflex-dock. A total of 20 poses were retained for each molecule. The post-docking processing was carried out using in-house shell scripts.

**Flexible Shape-Based Similarity Using Surflex-Sim.** The mutual alignment, carried out using four ligands, resulted in the most probable bioactive conformation of the selected ligands. The so-called bioactive conformation of Ro-64-6198 was used to carry out similarity-based enrichment studies. The Surflex-Sim module in SybylX 1.2 was used for the shape-based screening and enrichment of the ligand and decoy dataset. Twenty poses were retained, and the highest scoring pose was taken into consideration while evaluating the performance of the Surflex-Sim Similarity score. The ability of the program to extract seeded NOP agonists from the ligand+decoy set was calculated.

**Enrichment Factor Calculation and Effect of Similarity Search on Enrichment.** Enrichment factors were calculated to compare the performance of homology models as well as snapshots obtained from simulated annealing. A model is considered to be successful when the docking program ranks active ligands ahead of the decoy compounds. Enrichment curves are a useful tool to characterize the ability of a model to select active compounds and discard inactive compounds. Better models will rank active compounds more highly. Enrichment factors were used as a measure of the model's performance. Enrichment factors were calculated at 2%, 5%, and 10% of the database using the following equation

$$EF_{\text{subset}} = \frac{(\text{ligand}_{\text{selected}}/N_{\text{subset}})}{(\text{ligand}_{\text{total}}/N_{\text{total}})}$$

where  $\text{ligand}_{\text{total}}$  is the number of known ligands in a database containing  $N_{\text{total}}$  compounds, and  $\text{ligand}_{\text{selected}}$  is the number of ligands found in a given subset of  $N_{\text{subset}}$  compounds.  $EF_{\text{subset}}$  reflects the ability of virtual screening to find true positives among the decoys in the database compared to a random selection. Enrichment curves were obtained by plotting the percentage of actual ligands found (*Y*-axis) within the top ranked subset of all database compounds (*X*-axis). We also calculated a consensus score by combining the molecular docking scores in individual models and the similarity score using Surflex-Sim for each molecule in the decoy data set. Enrichment factors were calculated with the consensus scores for 2%, 5%, 10%, 15%, and 20% of the database using the above equation.

**Virtual Screening.** The virtual screening protocol was carried out in a tiered manner to increase the fidelity of the hits obtained. The tiered "Virtual Screening Funnel" is shown in Figure 2. The manually constructed pharmacophore, based on the binding conformation of Ro-2, was used to first screen the CNS Permeable subset of the ZINC database. This subset contains more than 400,000 small molecules which are prefiltered for CNS permeability.<sup>46</sup> The hits obtained after pharmacophore-based virtual screening (PBVS) were then subjected to a shape-based screening with Surflex-Sim, using the bioactive conformation of Ro-64-6198. These PBVS-filtered hits were then subjected to molecular docking with four different NOP receptor conformations (Models 01, 06, 08, and 11) selected from the enrichment studies. Molecular docking

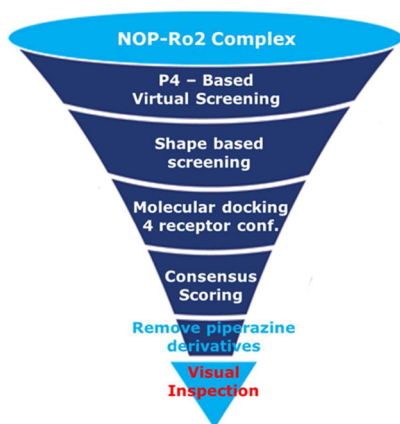


**Figure 2.** "Virtual Screening Funnel" depicting various steps used in virtual screening.

was performed using Surflex-Dock. A consensus score was calculated for each hit by totaling the Surflex-Sim and an average of four Surflex-Dock scores. Because piperazine rings are commonly found in CNS drugs and are likely to add to off-target effects, a further filtering step was performed to remove molecules containing a piperazine ring. The resulting compounds, ranked according to their consensus score, were inspected visually, and a set of 20 top-ranked compounds were purchased from their suppliers and tested for their binding affinity at the NOP receptor.

#### In Vitro Receptor Binding at Human NOP Receptors.

Binding to cell membranes was conducted in a 96-well format, as we have described previously.<sup>47</sup> Chinese hamster ovary (CHO) cells containing the human NOP receptor cDNA were grown in Dulbecco's Modified Eagle Medium (DMEM) with 10% fetal bovine serum in the presence of 0.4 mg/mL of G418 and 0.1% penicillin/streptomycin in 100 mm plastic culture dishes. For binding assays, the cells were scraped off the plate at confluence with a rubber policeman, homogenized in 50 mM Tris pH 7.5, using a Polytron homogenizer, and then centrifuged once and washed by an additional centrifugation at 27,000g for 15 min. The pellet was resuspended in Tris, and the suspension was incubated with [<sup>3</sup>H] N/OFQ (120 Ci/mmol, 0.2 nM) for binding to the NOPr. Nonspecific binding was determined with 1  $\mu$ M unlabeled N/OFQ. Total volume of incubation was 1.0 mL, and samples were incubated for 60 min at 25 °C. The amount of protein in the binding assay was 15  $\mu$ g. The reaction was terminated by filtration through glass fiber filters using a Tomtec 96 harvester (Orange, CT). Bound radioactivity was counted on a Pharmacia Biotech beta-plate liquid scintillation counter (Piscataway, NJ) and expressed in counts per minute. The first set of 20 compounds was tested at a single compound concentration of 300  $\mu$ M. For compounds that showed >50% displacement of radioligand binding at 300  $\mu$ M (Table 3), dose–response curves were determined in competition binding experiments with [<sup>3</sup>H] N/OFQ using at least six concentrations of each compound. The dose–response curves and  $IC_{50}$  values were generated using GraphPad/Prism (ISI, San Diego, CA).  $K_i$  values were calculated from the  $IC_{50}$  values by the method of Cheng and Prusoff.<sup>48</sup>

## RESULTS AND DISCUSSION

### Homology Models of the NOP Receptor Active-State and Inactive-State Conformations.

Separate homology models for the active-state and inactive-state conformations of the NOP receptor were built using the "Advanced Protein Modeling" module in SybylX 1.1. For details of the analysis of our models and comparison between active- and inactive-state conformations, the readers are guided to our previous paper.<sup>12</sup>

Being a member of class A GPCRs, the NOP model showed the expected topology of the 7TM helices. The root mean squared deviation of the initial active-state model with the template structure (opsin crystal structure 3CAP.pdb in this case) was found to be 2.27 Å. A higher deviation of the model structure was observed within the loop region. The comparison of the transmembrane helices revealed that the RMSD for the transmembrane helices was less than 0.5 Å. Side-chain bumps were removed by carrying out minimization. The RMSD of the final refined structure (after minimization) from the initial model was 1.065 Å (1.26 Å for inactive). The models were validated using PROCHECK and the ProSA Web server. The Ramachandran plots of the models suggested that 85.5% of the residues resided in the most favored regions in the active

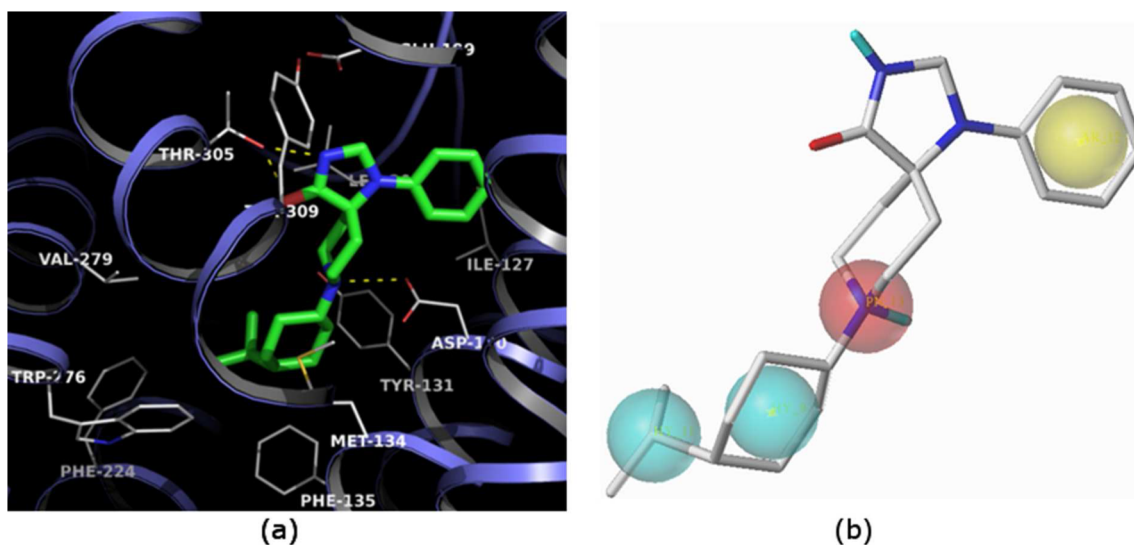


**Figure 3.** (a) Docked conformation of Ro-2 in the orthosteric binding site of active-state NOP receptor. Ro-2 is shown as green sticks, and the active site amino acids are shown in wire mode. (b) Manual pharmacophore defined using predicted bioactive conformation of Ro-2. Yellow sphere depicts an aromatic ring. Red sphere depicts a positively charged center, and two cyan spheres depict hydrophobic features.



**Figure 4.** Superposition of selected 12 active-state conformations of the NOP receptor after simulated annealing of the side-chains of the active site and EL2 loop.

conformation (83.3% for NOP in inactive conformation), 13.7% (13.7% for NOP in inactive conformation) in additionally allowed regions, and 0.8% (only two residues) (1.1% for NOP in inactive conformation) in the generously allowed regions. No residue was found in the disallowed regions in the active conformation, while about 5 residues (1.9%) were found in disallowed region in the inactive conformation. We also carried out 8 ns molecular dynamics simulations for the two models, as described in our previous communication. For details of the analysis of our models and comparison between active- and inactive-state conformations, the readers are guided to our previous paper.<sup>12</sup>

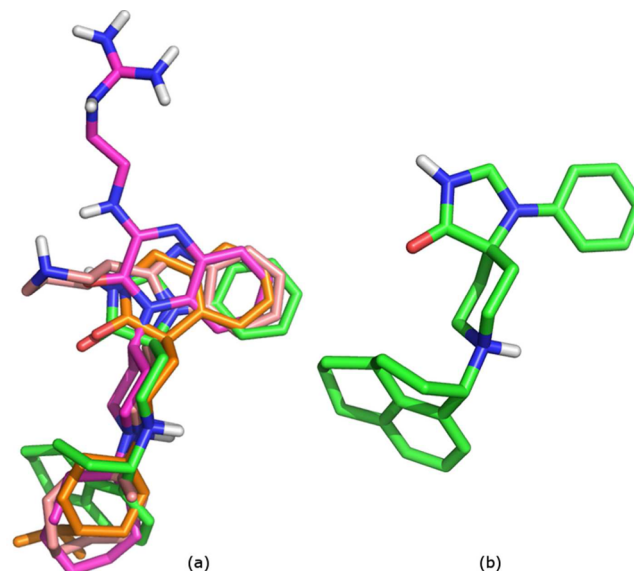


**Figure 5.** (a) Superposition of four selected ligands by Mutual Alignment "Hypothesis" obtained from Surflex-Sim. (b) Proposed bioactive conformation of Ro-64-6198 obtained from the Surflex-Sim "Hypothesis".

**Binding of Ro-2 to the NOP Receptor.** Molecular docking of the high-affinity NOP agonist ligand Ro-2 (**1**, Figure 1) into the binding site of the active-state NOP conformation resulted in a very high docking score (>10), suggesting high binding affinity toward the NOP receptor. The 1,3,8-triazaspiro[4.5]decan-4-one NOP agonists Ro-2 and Ro-64-6198 are highly selective NOP ligands. We have previously reported a binding mode of Ro-64-6198 at the active-state NOP receptor.<sup>12</sup> Ro-2 is bound to the NOP active site in a similar binding mode as Ro-64-6198. The aromatic ring of docked Ro-2 was surrounded by a hydrophobic surface from the side chains of the hydrophobic residues Cys200, Val202, Trp116, Val126, Ile127, and Leu104. As depicted in Figure 3a, this pocket is very small and may not accommodate bulky substitutions around this phenyl group. This is consistent

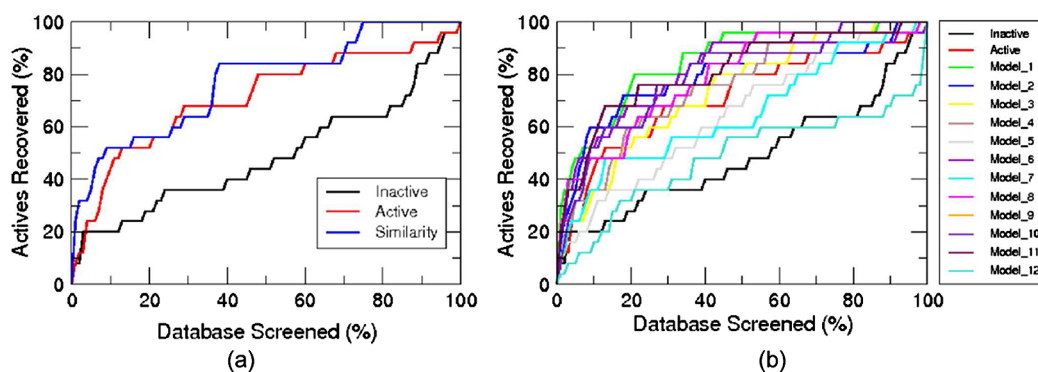


**Figure 6.** (a) Enrichment plots for nociceptin receptor homology models: inactive (black), active (red), and after similarity search (blue). (b) Enrichment plots for inactive and initial active homology models and selected 12 nociceptin receptor conformations after simulated annealing.

**Table 1. Enrichment Factors for Inactive and Initial Active Homology Model and Selected 12 Nociceptin Receptor Conformations after Simulated Annealing<sup>a</sup>**

model	2%	5%	10%
inactive	4.0	4.0	2.0
active	6.0	4.8	4.4
<b>Model_01</b>	<b>18.0</b>	<b>9.6</b>	<b>5.2</b>
<b>Model_02</b>	<b>12.0</b>	<b>7.2</b>	<b>6.0</b>
Model_03	6.0	4.8	3.6
<b>Model_04</b>	<b>12.0</b>	<b>6.4</b>	<b>3.6</b>
Model_05	6.0	3.2	2.8
<b>Model_06</b>	<b>12.0</b>	<b>8.8</b>	<b>5.2</b>
Model_07	6.0	4.8	3.6
<b>Model_08</b>	<b>14.0</b>	<b>8.0</b>	<b>4.8</b>
Model_09	8.0	6.4	5.2
Model_10	8.0	6.4	5.2
<b>Model_11</b>	<b>14.0</b>	<b>7.2</b>	<b>5.6</b>
Model_12	2.0	1.6	1.6

<sup>a</sup>Six active-state NOP models with the best enrichment factors are highlighted in bold.

with the experimental SAR reported by Wichmann et al.,<sup>27</sup> where substitutions other than a fluoro lead to a significant decrease in binding affinity for the NOP receptor.

The positively charged nitrogen of the piperidine ring was found to make the expected electrostatic interaction with the conserved Asp130. The hydrophobic moiety on the piperidine nitrogen (4-isopropyl-cyclohexyl group in case of Ro-2),<sup>39</sup>

responsible for conferring selectivity over other opioid receptors, is surrounded by hydrophobic amino acids such as Tyr131, Met134, Phe135, Ile219, Phe224, Trp276, and Val279. Among these residues, Ile219 is distinct from the corresponding residue (Val) in other three opioid receptors. This NOP hydrophobic pocket is wide enough to accommodate a variety of hydrophobic entities ranging from substituted cyclohexyl group (as in Ro-2) to tricyclic phenalen-1-yl (as in Ro 64-6198).

**Manual Pharmacophore of NOP Agonists.** The bioactive conformation of Ro-2 obtained from molecular docking was used to build a manual pharmacophore for NOP receptor binding. The extensive structure–activity relationship (SAR) data on the triazaspirodecanone series of NOP ligands available in the literature was used to define four pharmacophoric features represented in the NOP agonist Ro-2: (i) an aromatic ring, present in all the NOP agonists, (ii) a positively charged nitrogen atom, which makes a strong ionic interaction with the conserved Asp130 in the active site, (iii) and (iv) include hydrophobic groups proximal to the positively charged nitrogen atom. Hydrophobic substitutions on the piperidine ring nitrogen are known to be important requirements for binding of NOP ligands in the orthosteric site of the NOP receptor. Rover et al.<sup>39</sup> have reported that hydrophobic groups such as isopropyl or *t*-butyl on cycloalkyl substitutions on the ring nitrogen significantly improved potency and selectivity of these ligands toward the NOP receptor. Therefore, we included the fourth hydrophobic feature as a representative of these selectivity-contributing groups.

**Table 2. Enrichment Factors for an Inactive Model, Initial Active Homology Model, and Selected Nociceptin Receptor Conformations<sup>a</sup>**

model	enrichment				
	2%	5%	10%	15%	20%
inactive model	4.0 (8.0)	4.0 (4.8)	2.0 (2.4)	1.6 (2.7)	1.4 (2.0)
active model	6.0 (14.0)	4.8 (7.2)	4.4 (4.8)	3.5 (3.7)	2.6 (3.4)
<b>Model_01</b>	<b>18.0 (14.0)</b>	<b>9.6 (8.0)</b>	<b>5.2 (6.0)</b>	<b>4.0 (5.1)</b>	<b>3.8 (4.0)</b>
<b>Model_02</b>	<b>12.0 (14.0)</b>	<b>7.2 (6.4)</b>	<b>4.8 (6.0)</b>	<b>4.3 (5.1)</b>	<b>3.6 (3.8)</b>
<b>Model_06</b>	<b>12.0 (14.0)</b>	<b>8.8 (8.0)</b>	<b>5.2 (6.4)</b>	<b>5.1 (4.0)</b>	<b>3.4 (4.0)</b>
<b>Model_08</b>	<b>14.0 (14.0)</b>	<b>8.0 (5.6)</b>	<b>4.8 (4.4)</b>	<b>3.2 (4.3)</b>	<b>3.0 (3.8)</b>
<b>Model_09</b>	<b>8.0 (10.0)</b>	<b>6.4 (7.2)</b>	<b>5.2 (6.0)</b>	<b>4.0 (5.3)</b>	<b>3.0 (4.0)</b>
<b>Model_10</b>	<b>10.0 (8.0)</b>	<b>6.4 (7.2)</b>	<b>5.2 (6.0)</b>	<b>4.0 (5.3)</b>	<b>3.0 (4.0)</b>
<b>Model_11</b>	<b>14.0 (16.0)</b>	<b>7.2 (8.0)</b>	<b>5.6 (6.0)</b>	<b>4.5 (4.8)</b>	<b>8.4 (3.8)</b>

<sup>a</sup>The numbers in the parentheses indicate the enrichment factors after combined methods (consensus of shape-based and docking-based enrichment).

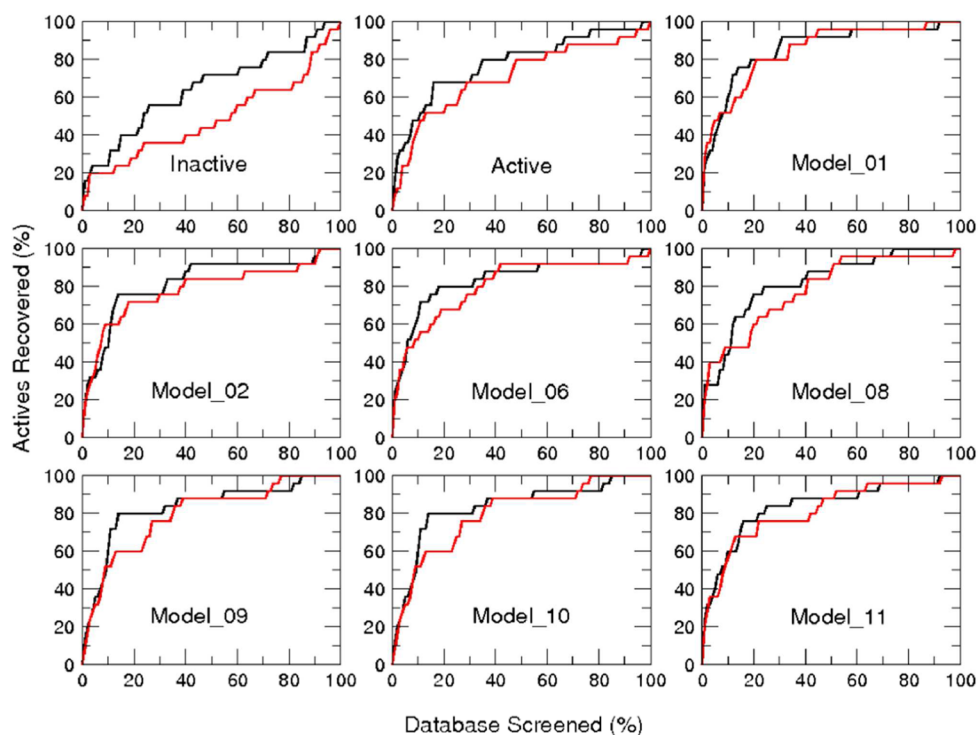


**Figure 7.** Enrichment plots for selected homology models (bold rows in Table 1) showing the percentage of the screened database (*X*-axis) vs the recovered active ligands (*Y*-axis). Red curve depicts the enrichment curve using docking, while the black curve illustrates the consensus (combined docking and shape-based approach) enrichment curve.

### Simulated Annealing To Define the Conformationally Flexible Extracellular Loop 2 (EL2) of the NOP Receptor.

The second extracellular loop in GPCRs plays an important role in the binding of small molecule ligands. It has also been shown to be of importance in the activation of the number of GPCRs. Typically, the receptor structure and active-site architecture of homology model-based GPCR structures are biased toward the template structure. In order to explore different possible orientations of active-site residues and possible conformations of the EL2 loop, we carried out simulated annealing of the EL2 loop and the transmembrane active site. The simulated annealing search resulted in 50 conformations of the active site of NOP. All conformations were energy-minimized and analyzed using PROCHECK. The active site residues were individually inspected for wrong geometries. The NOP-selective agonist Ro-2 was docked into the active site of the resultant conformations. On the basis of the binding mode and the docking score, 12 receptor conformations were selected, which differed considerably in the active site architecture. Figure 4 shows the overlay of the selected 12 active-state conformations of NOP receptor.

**Description of Small-Molecule Database (ZINC Subset) and Decoy Sets.** The quality of homology models is ultimately judged by their performance in docking and their ability to rank known ligands from a decoy set. The use of small-molecule decoy databases has been shown to be effective in enrichment studies using homology models. A drug-like decoy dataset can be generated containing small molecules with physicochemical properties similar to those of the seeded known ligands but with chemical diversity. The Directory of Useful Decoys (DUD) for 40 diverse targets was developed following these principles.<sup>49</sup> These datasets showed consistently higher enrichment in docking than an unbiased decoy dataset.

However, these datasets were of limited use in our study, as they differed significantly from the selected 25 NOP receptor agonists.

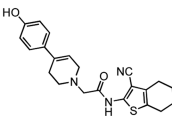
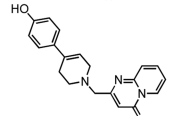
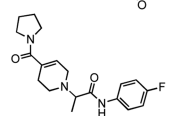
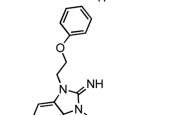
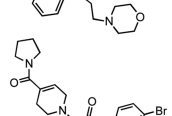
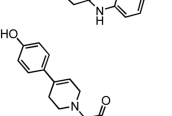
Hence, we constructed a library of decoys for our enrichment studies. Decoys were selected to ensure a ligand–decoy similarity of physicochemical properties, while imposing ligand–decoy chemical dissimilarity. Physicochemical properties similar to those of the seeded NOP ligands were within the following limit: (a) number of rings, 2–6; (b) molecular weight, 250–500; (c) number of rotatable bonds, 2–6; (d) cLogP, 2–4.9; (e) number of HBD, 1–3; and (f) number of HBA, 1–6.

**Description of Probable Bioactive Conformation Using Surflex-Sim Approach.** Four selected NOP ligands were aligned using Surflex-Sim to generate various “Hypothesis”. Each hypothesis represents probable bioactive conformations of the ligands in the most optimum alignment. The high scoring hypothesis showed compliance with the predicted binding conformation of Ro-64-6198.<sup>12</sup> As shown in Figure 5, the positively charged nitrogen atom and aromatic ring of the “A moiety” in the four ligands aligned well with each other. The putative bioactive conformation of Ro-64-6198 was selected for further analysis due to its minimum number of rotatable bonds, i.e., limited conformational flexibility.

**Enrichment Factor and Consensus Enrichment Factor Analysis. Enrichment Using Molecular Docking.** The database of 1000 small molecules (25 NOP ligands and 975 decoys) was used for the enrichment studies. Molecular docking of the seeded decoy database was carried out to assess the ability of the receptors (active-state and inactive-state) to retrieve seeded NOP ligands among the highly ranked compounds. The active-state conformation of the NOP receptor showed overall better enrichment than the inactive-



**Table 3. Selected Virtual Screening Hits That Showed >50% Inhibition of [<sup>3</sup>H] Nociceptin Binding in the Radioligand Binding Assays at the NOP Receptor at 300 μM<sup>a</sup>**

VS Hit	Structure	K <sub>i</sub> (μM) NOP Receptor
AT-1		23.01 ± 1.99
AT-2		49.17 ± 2.92
AT-3		>100
AT-4		1.42 ± 0.6
AT-5		34.55 ± 3.30
AT-6		39.69 ± 1.91
[ <sup>3</sup> H] nociceptin		0.00018 ± 0.00001

<sup>a</sup>K<sub>i</sub> values (from a dose–response experiment at six concentrations described in the Methods) are also shown.

state conformation (Figure 6). About 60% of the seeded NOP ligands were retrieved within the early 20% of the database by actNOP compared to only 25% by inactNOP. Interestingly, we found that NOP agonists gave higher docking scores than NOP antagonists when docked into the active-state NOP receptor homology models. NOP antagonists were therefore not used in this study. The binding of antagonists to the inactive-state of the receptor will be discussed in a future report.

Three out of the selected 12 active-state NOP models showed more than 70% recovery of seeded compounds in the top 20% of the ranked database. Out of the 12 models used, six models (Model\_01, \_02, \_04, \_06, \_08, and \_11) performed very well in the initial part of the screening, showing EF of more than 12 in the top 2% of the database, and had high EFs at 5% and 10% of database screened (Table 1). Overall, these models performed the best with good enrichment factors (above 7) even at 5% of the screened database. The remaining models showed moderate enrichment factors (3.5 to 5.0) at 10% of the ranked database. Model\_12 performed poorly in the virtual screens, showing low enrichment factors of 2.0, 1.6, and 1.6 at 2%, 5%, and 10% of the ranked database, respectively. The best performing models in the enrichment studies are highlighted in bold in Table 1.

Recently, Gatica and Cavasotto reported the construction of the GPCR Decoy Database (GDD) and evaluated the performance of docking at 19 GPCR targets.<sup>50</sup> The enrichment studies showed a marked decrease in the number of actives recovered from GDD, compared to bias-uncorrected

decoy sets where decoy molecules match the physicochemical properties of the ligand set. Our enrichment studies showed high enrichment rates despite using a NOP-specific decoy library (created as described in the Methods). These high enrichment factors suggest that the selected NOP receptor models possess high potential to identify NOP receptor agonists with high hit rates during virtual screening. Indeed, as discussed below, we obtained several micromolar affinity hits using these refined models for virtual screening.

**Enrichment Using Shape-Based Approach.** Mutual alignment of four selected diverse ligands in Surflex Sim resulted in probable bioactive conformations of the selected molecules. The shape-based screening of the seeded decoy library (containing 975 decoys and 25 NOP ligands) was carried out using molecular alignment. The shape-based approach resulted in higher enrichment, as shown in Figure 6a (blue curve). However, as shown in Figure 6a, the similarity-based enrichment curve showed considerable overlap with the docking-based enrichment using the active-state NOP receptor conformation.

**Enrichment Using Consensus Scores.** We compared the enrichment performance of the docking approach with the molecular alignment approach. The impact of using similarity search with Surflex-Sim on the docking-based enrichment was assessed. As shown in Table 2, enrichment factors significantly increased when combined with shape-based methods. The numbers in the parentheses indicate the enrichment factors after combined methods (consensus of shape-based and

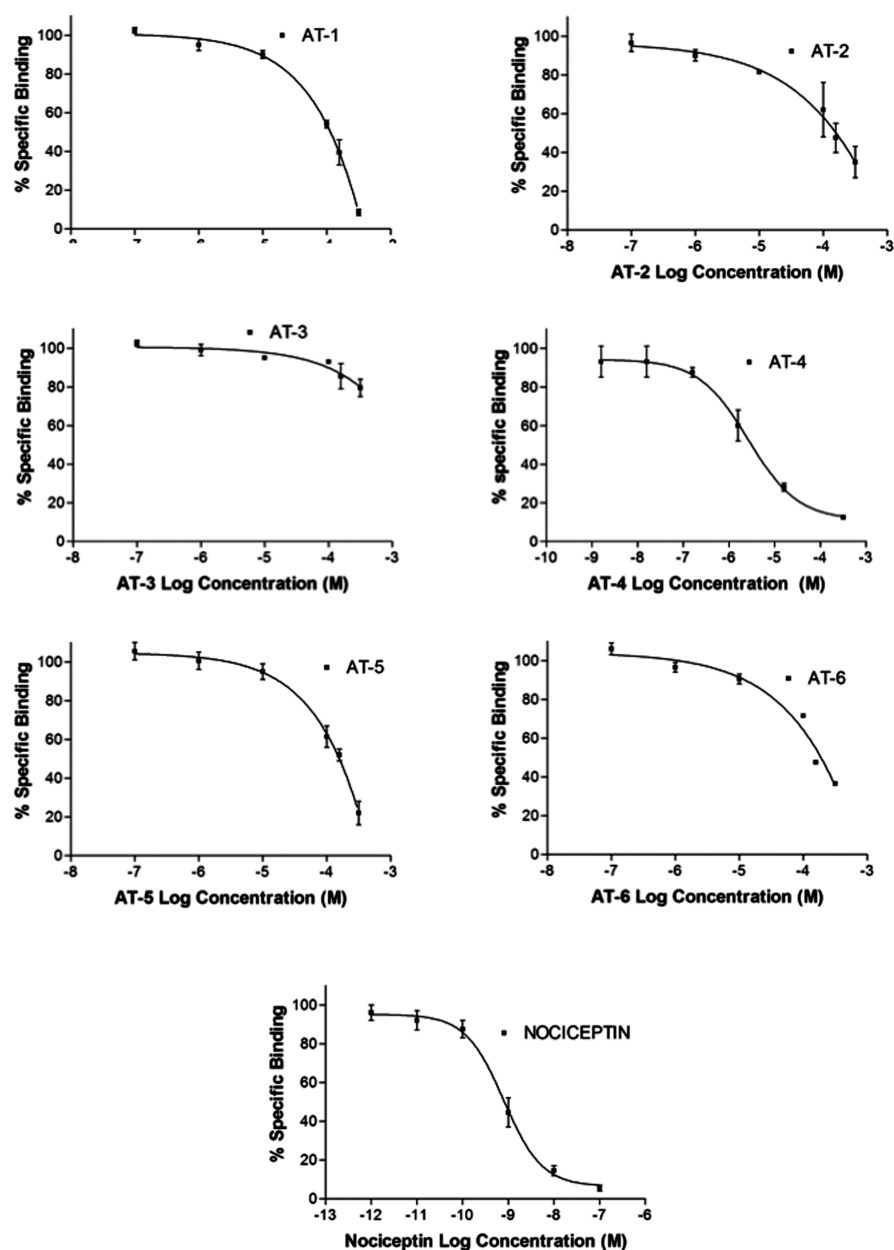


**Figure 8.** Dose–response binding curves for selected hit compounds from Table 3. These were determined by displacement of [ $^3\text{H}$ ]nociceptin binding to the NOP receptor by a range of concentrations of test compounds in competition binding experiments, as described in the Methods. The binding curves were generated using Prism (GraphPad, San Diego, CA). Each point represents the mean  $\pm$  S.E.M. determined in Prism ( $n = 3$ ). The  $\text{IC}_{50}$  values were determined by Prism from the binding curves and were used to derive the  $K_i$  values shown in Table 3 using the Cheng–Prusoff equation.<sup>48</sup>

docking-based enrichment). The enrichment curves of the selected models, which performed better with the above-mentioned consensus approach, are shown in the plots in Figure 7. Enrichment factors were higher when the two scoring methods were combined in 9 out of 13 models. As shown in Figure 7, the black curve representing the consensus enrichment curve shows higher EFs compared to the red curve representing enrichment by docking in individual receptor conformations.

**Virtual Screening.** The ultimate goal of the present study is to discover novel NOP ligands that can cross the blood–brain barrier. Hence, we used a “CNS Permeable” subset of ZINC, a free database, which contained more than 400,000 molecules. We used a two-stage approach for virtual screening. First, the

manual pharmacophore model, built using bioactive conformations, was used as a 3D query for screening the database, resulting in filtering of most of the compounds and generating a set of 2177 compounds for further screening by molecular docking. Using the average of four Surflex-Dock scores and the additive consensus score from the shape-based similarity score, this filtered set of 2177 molecules was further ranked, and the top 500 ranked compounds were grouped into a hit database. Piperazine-containing compounds were removed from these selected 500 compounds, resulting in a total of 240 compounds. After visual inspection of the remaining 240 compounds, 20 compounds representing two chemical series were selected for purchase and tested for their NOP binding affinity.

**Structure-Based Identification of a Novel Chemotype for the NOP Receptor.** Of the 240 compounds identified from the VS above, 20 compounds were purchased and tested for their binding affinity at the NOP receptor at a single concentration of 300  $\mu\text{M}$ . Six compounds from this set showed greater than 50% inhibition of [ $^3\text{H}$ ] nociceptin binding to the NOP receptor at 300  $\mu\text{M}$ . These were then further tested at a range of concentrations to obtain the binding affinity constant,  $K_i$ , at the NOP receptor (Table 3). The dose–response curves for the six compounds are shown in Figure 8.

Interestingly, one of the hit compounds, AT-4, had a 1.5  $\mu\text{M}$  binding affinity for the NOP receptor. From the six selected compounds, four compounds (AT-1, AT-4, AT-5, and AT-6) had binding affinities ( $K_i$ ) less than 50  $\mu\text{M}$  (Table 3). Compound AT-3, on the other hand, resulted in a binding affinity constant >100  $\mu\text{M}$  upon retesting in the dose–response experiments and was therefore not pursued further.

An ionic interaction with the conserved Asp130 in the binding pocket of the NOP receptor is a key anchoring binding event for all NOP ligands. A majority of the NOP ligands reported in the literature possess a positively charged nitrogen contained in a piperidine ring for this key pharmacophoric feature (Figures 1 and 3b). Our virtual screening uncovered a new chemical scaffold possessing this positively charged key pharmacophore distinct from the usual piperidine-containing NOP scaffolds, as shown in compound AT-4. Our results clearly demonstrate that our hybrid ligand- and structure-guided approach can result in identification of new chemical scaffolds within the screening set with binding affinity for the NOP receptor. Hit expansion and hit-to-lead optimization of these compounds is currently ongoing and will be reported in due course.

## CONCLUSIONS

The present work was designed to develop refined models of the active-state NOP receptor for use in VS to discover novel NOP binding chemotypes. We successfully built predictive models of the NOP receptor in active- as well as inactive-state conformations. Several active-state NOP conformations performed very well in enrichment studies using a bias-corrected ligand–decoy dataset. Furthermore, given that there is extensive SAR available on NOP ligands, we employed a hybrid approach for refinement and ranking of the NOP active-state receptor structures using a ligand-assisted shape-based method and a docking method. The combined docking-based and shape-based approach resulted in very high enrichment factors, indicating that the hybrid structure-based and ligand-based approach works better in the process of discovering relevant hits in a virtual screening campaign. The success of this hybrid approach was demonstrated by the identification of high affinity hits containing new chemical scaffolds from a virtual screening campaign and testing at the NOP receptor.

## AUTHOR INFORMATION

### Corresponding Author

\*Tel: 650-254-0786. Fax: 650-254-0787. E-mail: nurulain@astraeatherapeutics.com.

### Notes

The authors declare no competing financial interest.

## ACKNOWLEDGMENTS

This work was supported by funding from the National Institutes of Health NIDA R01DA014026, R01DA14026-07S1, and R01DA027811 to N.T.Z.

## REFERENCES

- (1) Chen, Y.; Fan, Y.; Liu, J.; Mestek, A.; Tian, M.; Kozak, C. A.; Yu, L. Molecular cloning, tissue distribution and chromosomal localization of a novel member of the opioid receptor gene family. *FEBS Lett.* **1994**, *347*, 279–83.
- (2) Bunzow, J. R.; Saez, C.; Mortrud, M.; Bouvier, C.; Williams, J. T.; Low, M.; Grandy, D. K. Molecular cloning and tissue distribution of a putative member of the rat opioid receptor gene family that is not a mu, delta or kappa opioid receptor type. *FEBS Lett.* **1994**, *347*, 284–8.
- (3) Mollereau, C.; Parmentier, M.; Mailleux, P.; Butour, J. L.; Moisand, C.; Chalon, P.; Caput, D.; Vassart, G.; Meunier, J. C. ORL1, a novel member of the opioid receptor family. Cloning, functional expression and localization. *FEBS Lett.* **1994**, *341*, 33–8.
- (4) Zaveri, N. Peptide and nonpeptide ligands for the nociceptin/orphanin FQ receptor ORL1: Research tools and potential therapeutic agents. *Life Sci.* **2003**, *73*, 663–78.
- (5) Bignan, G. C.; Connolly, P. J.; Middleton, S. A. Recent advances towards the discovery of ORL-1 receptor agonists and antagonists. *Expert Opin. Ther. Pat.* **2005**, *15*, 357–388.
- (6) Largent-Milnes, T. M.; Vanderah, T. W. Recently patented and promising ORL-1 ligands: where have we been and where are we going? *Expert Opin. Ther. Pat.* **2010**, *20*, 291–305.
- (7) Mustazza, C.; Bastanzio, G. Development of nociceptin receptor (NOP) agonists and antagonists. *Med. Res. Rev.* **2011**, *31*, 605–48.
- (8) Thompson, A. A.; Liu, W.; Chun, E.; Katritch, V.; Wu, H.; Vardy, E.; Huang, X. P.; Trapella, C.; Guerrini, R.; Calo, G.; Roth, B. L.; Cherezov, V.; Stevens, R. C. Structure of the nociceptin/orphanin FQ receptor in complex with a peptide mimetic. *Nature* **2012**, *485*, 395–9.
- (9) Negri, A.; Rives, M. L.; Caspers, M. J.; Prisinzano, T. E.; Javitch, J. A.; Filizola, M. Discovery of a novel selective kappa-opioid receptor agonist using crystal structure-based virtual screening. *J. Chem. Inf. Model.* **2013**, *53*, 521–6.
- (10) Lapalu, S.; Moisand, C.; Butour, J. L.; Mollereau, C.; Meunier, J. C. Different domains of the ORL1 and kappa-opioid receptors are involved in recognition of nociceptin and dynorphin A. *FEBS Lett.* **1998**, *427*, 296–300.
- (11) Mollereau, C.; Mouldous, L.; Lapalu, S.; Cambois, G.; Moisand, C.; Butour, J. L.; Meunier, J. C. Distinct mechanisms for activation of the opioid receptor-like 1 and kappa-opioid receptors by nociceptin and dynorphin A. *Mol. Pharmacol.* **1999**, *55*, 324–31.
- (12) Daga, P. R.; Zaveri, N. T. Homology modeling and molecular dynamics simulations of the active state of the nociceptin receptor reveal new insights into agonist binding and activation. *Proteins* **2012**, *80*, 1948–61.
- (13) Ronzoni, S.; Peretto, I.; Giardina, G. A. M. Lead generation and lead optimization approaches in the discovery of selective, non-peptide ORL-1 receptor agonists and antagonists. *Expert Opin. Ther. Pat.* **2001**, *11*, 525–546.
- (14) Bignan, G. C.; Battista, K.; Connolly Peter, J.; Orsini Michael, J.; Liu, J.; Middleton Steven, a.; Reitz Allen, B. 3-(4-Piperidinyl)indoles and 3-(4-piperidinyl)pyrrolo-2,3-b pyridines as ligands for the ORL-1 receptor. *Bioorg. Med. Chem. Lett.* **2006**, *16*, 3524–8.
- (15) Zaveri, N. T.; Jiang, F.; Olsen Cris, M.; Deschamps Jeffrey, R.; Parrish, D.; Polgar, W.; Toll, L. A novel series of piperidin-4-yl-1,3-dihydroindol-2-ones as agonist and antagonist ligands at the nociceptin receptor. *J. Med. Chem.* **2004**, *47*, 2973–6.
- (16) Zaveri, N.; Jiang, F.; Olsen, C.; Polgar, W.; Toll, L. Small-molecule agonists and antagonists of the opioid receptor-like receptor (ORL1, NOP): Ligand-based analysis of structural factors influencing intrinsic activity at NOP. *AAPS J.* **2005**, *7*, E345–52.
- (17) Cheng, T.; Li, Q.; Zhou, Z.; Wang, Y.; Bryant, S. H. Structure-based virtual screening for drug discovery: A problem-centric review. *AAPS J.* **2012**, *14*, 133–41.

- (18) Koshland, D. E. Application of a theory of enzyme specificity to protein synthesis. *Proc. Natl. Acad. Sci. U.S.A.* **1958**, *44*, 98–104.
- (19) Boehr, D. D.; Nussinov, R.; Wright, P. E. The role of dynamic conformational ensembles in biomolecular recognition. *Nat. Chem. Biol.* **2009**, *5*, 789–96.
- (20) Sherman, W.; Beard, H. S.; Farid, R. Use of an induced fit receptor structure in virtual screening. *Chem. Biol. Drug Des.* **2006**, *67*, 83–4.
- (21) Cozzini, P.; Kellogg, G. E.; Spyraakis, F.; Abraham, D. J.; Costantino, G.; Emerson, A.; Fanelli, F.; Gohlke, H.; Kuhn, L. A.; Morris, G. M.; Orozco, M.; Pertinhez, T. A.; Rizzi, M.; Sotriffer, C. A. Target flexibility: An emerging consideration in drug discovery and design. *J. Med. Chem.* **2008**, *51*, 6237–55.
- (22) Osguthorpe, D. J.; Sherman, W.; Hagler, A. T. Generation of receptor structural ensembles for virtual screening using binding site shape analysis and clustering. *Chem. Biol. Drug Des.* **2012**, *80*, 182–93.
- (23) Cavasotto, C. N.; Kovacs, J. A.; Abagyan, R. A. Representing receptor flexibility in ligand docking through relevant normal modes. *J. Am. Chem. Soc.* **2005**, *127*, 9632–40.
- (24) Rueda, M.; Bottegoni, G.; Abagyan, R. Consistent improvement of cross-docking results using binding site ensembles generated with elastic network normal modes. *J. Chem. Inf. Model.* **2009**, *49*, 716–25.
- (25) Vilar, S.; Costanzi, S. Application of Monte Carlo-based receptor ensemble docking to virtual screening for GPCR ligands. *Methods Enzymol.* **2013**, *522*, 263–78.
- (26) Nichols, S. E.; Baron, R.; Ivetac, A.; McCammon, J. A. Predictive power of molecular dynamics receptor structures in virtual screening. *J. Chem. Inf. Model.* **2011**, *51*, 1439–46.
- (27) Wichmann, J.; Adam, G.; Rover, S.; Hennig, M.; Scalone, M.; Cesura, A. M.; Dautzenberg, F. M.; Jenck, F. Synthesis of (1S,3aS)-8-(2,3,3a,4,5,6-hexahydro-1H-phenalen-1-yl)-1-phenyl-1,3,8-triazaspiro[4.5]decan-4-one, a potent and selective orphanin FQ (OFQ) receptor agonist with anxiolytic-like properties. *Eur. J. Med. Chem.* **2000**, *35*, 839–51.
- (28) Rover, S.; Adam, G.; Cesura, A. M.; Galley, G.; Jenck, F.; Monsma, F. J., Jr.; Wichmann, J.; Dautzenberg, F. M. High-affinity, non-peptide agonists for the ORL1 (orphanin FQ/nociceptin) receptor. *J. Med. Chem.* **2000**, *43*, 1329–38.
- (29) Caldwell, J. P.; Matasi, J. J.; Zhang, H.; Fawzi, A.; Tulshian, D. B. Synthesis and structure-activity relationships of N-substituted spiropiperidines as nociceptin receptor ligands. *Bioorg. Med. Chem. Lett.* **2007**, *17*, 2281–2284.
- (30) Caldwell, J. P.; Matasi Julius, J.; Fernandez, X.; McLeod Robbie, L.; Zhang, H.; Fawzi, A.; Tulshian Deen, B. Synthesis and structure-activity relationships of N-substituted spiropiperidines as nociceptin receptor ligands: part 2. *Bioorg. Med. Chem. Lett.* **2009**, *19*, 1164–7.
- (31) Mustazza, C.; Borioni, A.; Sestili, I.; Sbraccia, M.; Rodomonte, A.; Del Giudice, M. R. Synthesis and pharmacological evaluation of 1,2-dihydrospiro[isoquinoline-4(3H),4'-piperidin]-3-ones as nociceptin receptor agonists. *J. Med. Chem.* **2008**, *51*, 1058–1062.
- (32) Palin, R.; Bom, A.; Clark, J. K.; Evans, L.; Feilden, H.; Houghton, A. K.; Jones, P. S.; Montgomery, B.; Weston, M. A.; Wishart, G. Synthesis and evaluation of N-3 substituted phenoxypropyl piperidine benzimidazol-2-one analogues as NOP receptor agonists with analgesic and sedative properties. *Bioorg. Med. Chem.* **2007**, *15*, 1828–1847.
- (33) Palin, R.; Clark John, K.; Evans, L.; Houghton Andrea, K.; Jones Philip, S.; Prosser, A.; Wishart, G.; Yoshiizumi, K. Structure-activity relationships and CoMFA of N-3 substituted phenoxypropyl piperidine benzimidazol-2-one analogues as NOP receptor agonists with analgesic properties. *Bioorg. Med. Chem. Lett.* **2008**, *16*, 2829–51.
- (34) Goehring, R. R.; Matsumira, A.; Shao, B.; Taoda, Y.; Tsuno, N.; Whitehead, J. W. F.; Yao, J. Substituted Quinoxaline-Type Piperidine Compounds and the Uses Thereof, Patent Application CA 2730288 A1, 2009.
- (35) Ho, G. D.; Anthes, J.; Bercovici, A.; Caldwell, J. P.; Cheng, K. C.; Cui, X.; Fawzi, A.; Fernandez, X.; Greenlee, W. J.; Hey, J.; Korfmacher, W.; Lu, S. X.; McLeod, R. L.; Ng, F.; Torhan, A. S.; Tan, Z.; Tulshian, D.; Varty, G. B.; Xu, X.; Zhang, H. The discovery of tropane derivatives as nociceptin receptor ligands for the management of cough and anxiety. *Bioorg. Med. Chem. Lett.* **2009**, *19*, 2519–23.
- (36) Ho, G. D.; Bercovici, A.; Tulshian, D.; Greenlee, W. J.; Fawzi, A.; Fernandez, X.; McLeod, R. L.; Smith Torhan, A.; Zhang, H. Synthesis and structure-activity relationships of 4-hydroxy-4-phenylpiperidines as nociceptin receptor ligands: Part 2. *Bioorg. Med. Chem. Lett.* **2007**, *17*, 3028–3033.
- (37) Ho, G. D.; Bercovici, A.; Tulshian, D.; Greenlee, W. J.; Fawzi, A.; Smith Torhan, A.; Zhang, H. Synthesis and structure-activity relationships of 4-hydroxy-4-phenylpiperidines as nociceptin receptor ligands: Part 1. *Bioorg. Med. Chem. Lett.* **2007**, *17*, 3023–3027.
- (38) Irwin, J. J.; Sterling, T.; Mysinger, M. M.; Bolstad, E. S.; Coleman, R. G. ZINC: A free tool to discover chemistry for biology. *J. Chem. Inf. Model.* **2012**, *52*, 1757–68.
- (39) Rover, S.; Wichmann, J.; Jenck, F.; Adam, G.; Cesura, A. M. ORL1 receptor ligands: Structure-activity relationships of 8-cycloalkyl-1-phenyl-1,3,8-triazaspiro[4.5]decan-4-ones. *Bioorg. Med. Chem. Lett.* **2000**, *10*, 831–4.
- (40) Jain, A. N. Surflex-Dock 2.1: Robust performance from ligand energetic modeling, ring flexibility, and knowledge-based search. *J. Comput. Aided Mol. Des.* **2007**, *21*, 281–306.
- (41) Meng, F.; Taylor, L. P.; Hoversten, M. T.; Ueda, Y.; Ardati, A.; Reinscheid, R. K.; Monsma, F. J.; Watson, S. J.; Civelli, O.; Akil, H. Moving from the orphanin FQ receptor to an opioid receptor using four point mutations. *J. Biol. Chem.* **1996**, *271*, 32016–20.
- (42) Meng, F.; Ueda, Y.; Hoversten, M. T.; Taylor, L. P.; Reinscheid, R. K.; Monsma, F. J.; Watson, S. J.; Civelli, O.; Akil, H. Creating a functional opioid alkaloid binding site in the orphanin FQ receptor through site-directed mutagenesis. *Mol. Pharmacol.* **1998**, *53*, 772–7.
- (43) Mouldous, L.; Topham, C. M.; Moisan, C.; Mollereau, C.; Meunier, J. C. Functional inactivation of the nociceptin receptor by alanine substitution of glutamine 286 at the C terminus of transmembrane segment VI: evidence from a site-directed mutagenesis study of the ORL1 receptor transmembrane-binding domain. *Mol. Pharmacol.* **2000**, *57*, 495–502.
- (44) Peeters, M. C.; van Westen, G. J.; Guo, D.; Wisse, L. E.; Muller, C. E.; Beukers, M. W.; Ijzerman, A. P. GPCR structure and activation: An essential role for the first extracellular loop in activating the adenosine A2B receptor. *FASEB J.* **2011**, *25*, 632–43.
- (45) Shi, L.; Javitch, J. A. The second extracellular loop of the dopamine D2 receptor lines the binding-site crevice. *Proc. Natl. Acad. Sci. U.S.A.* **2004**, *101*, 440–5.
- (46) Pajouhesh, H.; Lenz, G. R. Medicinal chemical properties of successful central nervous system drugs. *NeuroRx* **2005**, *2*, 541–53.
- (47) Zaveri, N.; Polgar, W. E.; Olsen, C. M.; Kelson, A. B.; Grundt, P.; Lewis, J. W.; Toll, L. Characterization of opiates, neuroleptics, and synthetic analogs at ORL1 and opioid receptors. *Eur. J. Pharmacol.* **2001**, *428*, 29–36.
- (48) Cheng, Y.; Prusoff, W. H. Relationship between the inhibition constant ( $K_i$ ) and the concentration of inhibitor which causes 50% inhibition ( $I_{50}$ ) of an enzymatic reaction. *Biochem. Pharmacol.* **1973**, *22*, 3099–108.
- (49) Huang, N.; Shoichet, B. K.; Irwin, J. J. Benchmarking sets for molecular docking. *J. Med. Chem.* **2006**, *49*, 6789–801.
- (50) Gatica, E. A.; Cavasotto, C. N. Ligand and decoy sets for docking to G protein-coupled receptors. *J. Chem. Inf. Model.* **2012**, *52*, 1–6.